

DOSIMETRY FOR RADIOBIOLOGICAL STUDIES USING  
HIGH ENERGY PARTICLE BEAMS

A.H. Sullivan and J. Baarli

A B S T R A C T

The methods used to estimate the absorbed dose to biological objects irradiated in high energy neutron, proton and pion beams are described. The limitations of tissue-equivalent ionization chambers when used for high energy particle dosimetry are discussed and an estimation of the correction required is given. Depth-dose curves are presented and dosimetry problems associated with the spatial distribution of the dose are considered. It is concluded that absorbed dose to a biological object in a high energy particle beam can be estimated to within about 10%.

1. INTRODUCTION

High energy particles produce a range of nuclear interaction products when they interact with a nucleus, which deposit energy in a different pattern than do conventional energy radiations. Hence the study of the biological effect of high energy particle radiation is of interest to see if nuclear interactions have any special significance. Also unstable particle beams such as positive and negative pions, should be investigated experimentally in order to provide data with which to judge the possible application of such beams when higher intensities become available.

There are a number of parameters which characterize a high energy particle beam, which may be determined and may be of interest for the understanding of radiobiological effects. However, the common denominator, when comparing the effects of different radiations is, by convention, taken to be the absorbed dose or the macroscopic energy absorption per unit mass and the primary effort in high energy particle beam dosimetry is devoted to determining this quantity.

To be presented at IAEA Symposium on Dosimetric Techniques  
as applied to Agriculture, Industry, Biology and Medicine  
Vienna, 17-21 April, 1972

2. HIGH ENERGY PARTICLE BEAMS AVAILABLE AT CERN

Beams for radiobiological studies<sup>(1)</sup> are produced using the CERN 600 MeV Synchro-cyclotron. The beams of principal interest are the extracted primary proton beam of 600 MeV and the secondary neutron and pion beams produced when the protons interact with an internal target. The layout of the machine and the beam lines of interest are shown in Fig. 1. The proton beam is used in an underground beam tunnel and its intensity and diameter can be varied over a wide range<sup>(2)</sup>. The neutron beam is produced in the forward direction from the internal proton beam interacting with a beryllium target. The neutrons have an energy distribution with a maximum of 400 MeV<sup>(3)</sup>. The diameter of the beam is controlled by the size of the beam channel through the shielding wall<sup>(4)</sup>. Positive and negative pions are obtained when the beryllium target is suitably placed in the machine such that the magnetic field of the cyclotron deflects particles of the required charge and momentum into the beam aperture<sup>(5)</sup>. The properties of the beams are given in Table I. As can be seen the dose-rates obtainable with the secondary beams are very low and only a limited range of radiobiological experiments are possible. Dose-rate in the beams as a function of depth in water is shown in Fig. 2. The dose in the 400 MeV neutron beam rapidly builds up as the neutrons interact and knock out fast protons in the forward direction. The dose at the front surface of the absorber is principally due to short-range products from nuclear interactions; this component of the dose is diluted with proton ionization as the depth increases until equilibrium is reached at about 18 g/cm<sup>2</sup> depth. The pion depth-dose curves show the characteristic Bragg stopping peak for charged particles; however, the positive pion peak also contains the energy dissipated in the pion to muon to positron decay. The negative pion peak contains the locally deposited energy following pion capture. The pion curves shown are for the same initial energy pions, which therefore have the same range, and the difference in shape of the depth-dose curves roughly indicates the region where the excess energy due to negative pion capture is deposited. Behind the main pion peak is seen the contribution of contaminating muons and electrons.

With 600 MeV protons there is a rapid initial dose build-up as electronic equilibrium is established, then a slower build-up of dose with depth due to nuclear interactions; the dose then decreases as protons get scattered out of the primary beam and eventually a Bragg peak is found at about 1.5 m depth.

### 3. MEASUREMENT OF DOSE OF HIGH ENERGY PARTICLES

Absorbed dose to biological samples irradiated in the beams is determined using tissue-equivalent ionization chambers. Ideally the dosimeter should have small dimensions so that it can be used to measure the dose at a point in situations where dose is a strong function of position. However, some compromise in the design of the chamber has to be made in order to get sufficient sensitivity to measure the low dose-rates in the available beams. Two chambers are used, both have parallel-plate electrodes made of tissue-equivalent plastic<sup>(6)</sup> and are filled with tissue-equivalent gas<sup>(7)</sup>. One chamber has a 3 mm plate spacing and 6 cm diameter collector and is used when the beam diameter is large and it is required to know precisely the depth at which the sensitive volume is situated in an absorber. The other chamber has a 20 mm diameter electrode and 23 mm spacing and is intended for the measurement of average dose over volumes of the order of 1 cm radius. The construction of the 20 mm chamber is shown in Fig. 3. The chambers are in an aluminium pressure casing and the gas pressure can be varied. The chambers have an entrance window of total mass 570 mg/cm<sup>2</sup>. The dosimeters are calibrated against Co-60 gamma rays from a source that has been compared with a standard radium source. The Co-60 calibration of the chambers agrees with that calculated if a value of  $\omega$  of 31.6 eV per ion pair is used.

The dose from high energy particles arises from the normal slowing down ionization if the particles are charged, and from the products of nuclear interactions in the material through which they pass. Tissue-equivalent materials have a composition that is adjusted to have the same average electron density and hydrogen concentration as muscle, such that gamma-ray and fast neutron interactions reasonably represent those in actual tissue. High energy particle inelastic cross-sections on the

other hand are a function of atomic weight, and the distribution of energy between the fragments that result from an interaction depend on nuclear structure. Hence the replacement of oxygen by carbon, which is normal in electrically conducting tissue-equivalent plastics, can be expected to have an effect on the response of a tissue-equivalent dosimeter to high energy particles.

The dose-rate is obtained from the ionization current produced in the chambers by a relation:

$$D = S f_1 f_2 \frac{i}{P} \text{ rad/h} .$$

where  $S$  is the sensitivity determined from calibration and has values of 1.24 and 1.28 rad/h for the 3 mm and 23 mm spacing chambers respectively when  $i$  is the output current in picoamperes and  $P$  the absolute gas pressure in  $\text{kg/cm}^2$  at  $20^\circ\text{C}$ .

$f_1$  is a correction factor to allow for the non-tissue-equivalence of the chambers when used for estimating the dose to soft tissue. For neutrons the factor allows for the difference in macroscopic cross-section between the chamber material and tissue and the dose correction factor has a value:

$$f_1 = (1 - 0.05 \frac{D_0}{D})$$

where  $D_0$  is the dose in the beam extrapolated to zero absorber depth, and  $D$  the dose to be corrected. For stopped negative pions a correction is necessary on account of the differences in energy carried off by long-range secondaries<sup>(8)</sup>. A correction factor of 0.95 is estimated for this case. The correction will be insignificant in charged particle beams.

$f_2$  is a correction factor for the efficiency of the chamber and includes initial recombination ionization loss and any change in the value for  $\omega$ , the energy expended per ion pair. The value for  $\omega$  is not expected to be increased by more than 1% for the ionization produced in high energy particle beams. Recombination corrections must be estimated for the conditions under which the dosimeter is

used and typically make a 4% correction for the 23 mm spacing chamber in the stopped pion region and is insignificant for the 3 mm chamber when used with 300 V polarizing supply.

Irradiations in the proton beam can be made at dose-rates up to a kilorad per minute. High dose-rate measurements are made with a 0.6 cc air-equivalent ionization chamber which is placed in a phantom at the point at which biological exposures are to be made. Delta rays from the protons have a maximum range of several mm in plastic. As the chamber wall is only 0.5 mm thick, the material surrounding the chamber will have some influence on the dose estimation. The chamber is calibrated with Co-60 gamma rays. If the ionization current is  $i_0$  per roentgen/h of Co-60 gamma rays, then a measured current  $i$ , when the chamber is in a beam of 600 MeV protons, will be an indication of a dose-rate  $D$  rad/h given by:

$$D = 0.83 \frac{i}{i_0} \frac{(S_t)}{(S_a)} \cdot f = 0.95 \frac{i}{i_0} f$$

$S_t$  and  $S_a$  are the stopping powers of 600 MeV protons in tissue and air.  $f$  is a calculated correction factor taking into account the effect of the surrounding medium and has values given in the table below.

Surrounding material	f
Lucite	0.98
Polythene	0.96
Carbon	1.0
Aluminium	1.02

Dose-rate estimations using the air-equivalent chamber satisfactorily compare with those from tissue-equivalent chambers at low dose-rates.

Particle flux densities in the proton and neutron beams are estimated from the activation of Carbon-12. A plastic scintillator

is exposed in the beam and the resulting Carbon-11 activity, produced by  $^{12}\text{C}(n,2n)^{11}\text{C}$  or  $^{12}\text{C}(p,np)^{11}\text{C}$  reactions is counted by placing the scintillator on a photomultiplier. The 20.4 min half-life positron activity gives a measure of the particle flux above the reaction threshold of 20 MeV.

#### 4. DETERMINATION OF DOSE TO A BIOLOGICAL SPECIMEN

It is of interest to radiobiology to find the radiation effectiveness associated with different interaction processes. For this reason irradiations are made at different absorber depths in a high energy particle field where the secondary particle spectrum contributing to the dose may be completely different even for the same beam. An example of this is the negative pion beam where nuclear interactions are important only at the end of the pion range.

Dose measurements in the secondary beams are made with the 20 mm and 60 mm diameter tissue-equivalent chambers that have already been described, from which the dose to actual biological objects such as mice testes and eye lens, and Vicia Faba root-tips has to be estimated. At the peaks in the pion beams the dose is varying with position in all three directions. Dose contours across the beam profile at the exposure position are determined from an X-ray film exposure. Normal beam focusing is such that the beam half-widths are of the order of 5 cm and at 1 cm radius the beam intensity is 85% of that on the centre line<sup>(9)</sup>. The peak in the pion depth-dose curve typically drops by about 15% at  $1 \text{ g/cm}^2$  from the maximum in the peak. Hence the dose at any point within about  $1 \text{ g/cm}^2$  of the position of maximum value will not differ from the average value measured with the 20 mm diameter chamber by more than about  $\pm 15\%$ . The experimental set-up for irradiating mice testes with positive and negative pions is shown in Fig. 4. A depth-dose curve is first made over the peak region. The mouse cage holder is positioned by using a phantom in the cage with a 0.6 cc ionization chamber at the position of the testes. Absorber thickness and holder position are adjusted until a maximum reading is obtained. Also shown in Fig. 4 is the beam monitor ionization chamber through which the whole beam passes and which is used to

control the biological exposures. A small correction to the dose is necessary to account for the fact that the mice are not hard against the absorber; this correction is determined experimentally and is normally about 4%.

Procedures using similar principles have been worked out for the other beams and for other types of biological irradiations<sup>(9,10)</sup>.

## 5. DISCUSSION

The problems of dosimetry of high energy particle beams differ from those normally encountered in radiobiological dosimetry. The differences are on account of the inelastic nuclear interactions that are caused by high energy particles and which result in relatively large amounts of energy being deposited in a relatively small volume. This energy has been estimated and is on average about 20 MeV deposited locally from a pion interaction and about 17 MeV from a high energy neutron interaction. The 20 MeV from pion interactions should be compared with the 130 MeV rest mass of the pion that is dissipated. The major part of this energy goes into neutrons, long-range protons and excitations. The composition of the dose and the secondary particle distribution in high energy particle beams varies rapidly with absorber depth and the dosimeter has to respond correctly over this range of variation. The corrections that are necessary to adjust defects in the response of the dosimeters are fortunately small as they cannot be calculated with any precision and are expected to depend on beam diameter as well as depth in the absorber. The practical difficulty of determining the dose over a small region where the dose is varying with position, and then of placing the biological sample at this point is probably a more serious limitation than any systematic error due to inaccurate corrections to the readings of the dosimeters used.

Although absorbed dose is the parameter required for the inter-comparison of radiation effectiveness, the understanding of radiobiological processes that occur with high energy particle beams would need a more detailed description of the radiation field and the interactions that take place. The parameter most easily determined is the

high energy particle flux density. The high energy particle flux density in an absorber varies only slowly with depth, the flux density as measured by carbon activation increases by about 20% over the first 20 cm depth of water in the proton and neutron beams due to the production of secondary particles capable of activating carbon, and then slowly decreases. As the flux density of high energy particles is proportional to the nuclear interaction rate, this quantity is probably as important as absorbed dose from the point of view of the interpretation of radiobiological effects.

As estimation of the precision of a dose determination is a matter of conjecture in view of all the possible sources of error. With the dosimetry system at present employed, an estimation of the absorbed dose to a biological object in a high energy particle beam is thought to be within less than  $\pm 10\%$  of the true value.



REFERENCES

- (1) BAARLI, J., et al., Int. Congr. Protection against Accelerator and Space Radiation (Proc. Conf. CERN Geneva, 1971) 133.
- (2) LAMB, M.J., et al., The mutagenic effect of 600 MeV protons in *Drosophila Melanogaster*, Int. J. Rad. Biol. 12 1 (1967) 27.
- (3) ARMSTRONG, T.W., BISHOP, B.L., Calculation of the absorbed dose and dose equivalent induced by medium-energy neutrons, protons and comparison with experiment, Rad. Res. 47 (1971) 581.
- (4) BAARLI, J., SULLIVAN, A.H., Dosimetry studies of a high-energy neutron beam, Phys. Med. Biol., 14 2 (1969) 269.
- (5) SULLIVAN, A.H., BAARLI, J., Some measurements on the slowing down of  $\pi$  mesons in tissue-equivalent material, Phys. Med. Biol., 13 3 (1968) 435.
- (6) SHONKA, F.R., et al., Int. Conf. peaceful Uses of atom. Energy (Proc. Conf. Geneva, 1958) 21, UN, New York (1958) 184.
- (7) ROSSI, H.H., "Radiation Dosimetry", Ch. 15-111 B, Neutrons and Mixed Radiations (HINE, G.J., BROWNELL, G.L., eds.), Academic Press (1956).
- (8) GUTHRIE, M.P., et al., Calculation of the capture of negative pions in light elements and comparison with experiments pertaining to cancer radiotherapy, Nucl. Inst. Meth., 66 (1968) 29.
- (9) BAARLI, J., et al., An estimation of the RBE of stopped pions from observations of spermatogonia survival in mice, Int. J. Rad. Biol., 19 6 (1971) 537.
- (10) Di PAOLA, M., et al., Int. Congr. Protection against Accelerator and Space Radiation (Proc. Conf. CERN Geneva, 1971) 102.

FIGURE CAPTIONS

- Figure 1. Layout of the 600 MeV CERN Synchro-cyclotron showing beam lines used for radiobiology.
- Figure 2. Absorbed dose as a function of depth in water in beams that have been used for radiobiology. The curves are normalized at a depth of 1 g/cm<sup>2</sup>.
- Figure 3. Construction of tissue-equivalent ionization chamber used for dose measurement in high energy particle beams.
- Figure 4. The experimental arrangement for the irradiation of mice with stopped pions. The beam monitor is on the left, then the absorber with mouse holder attached. A small ionization chamber inside a mouse phantom is shown at the irradiation position.

Table I

Beams from 600 MeV Synchro-cyclotron  
used for radiobiology

	Energy (MeV)	Beam strength	Useful diameter (cm)	Dose-rate at 1 g/cm <sup>2</sup> (rad/h)	Dose-rate at max.build-up (rad/h)	Depth of max. dose-rate (g/cm <sup>2</sup> )	Contami- nation
Protons	600	10 <sup>8</sup> -10 <sup>11</sup> /sec	14	50-50,000	60-60,000	10	Small
Neutrons	400 max.	3.5x10 <sup>5</sup> /cm <sup>2</sup> /sec	18	6	10	20	<8% gamma contribution to dose at 1 g/cm <sup>2</sup>
Pions †	80-110	4x10 <sup>5</sup> /sec	2	Dose-rate 4 rad/h over volume 2 cm diameter in stopping region			10% of peak dose-rate from muons + electrons

CERN 600 MeV Synrocyclotron - Beams used for radiobiology

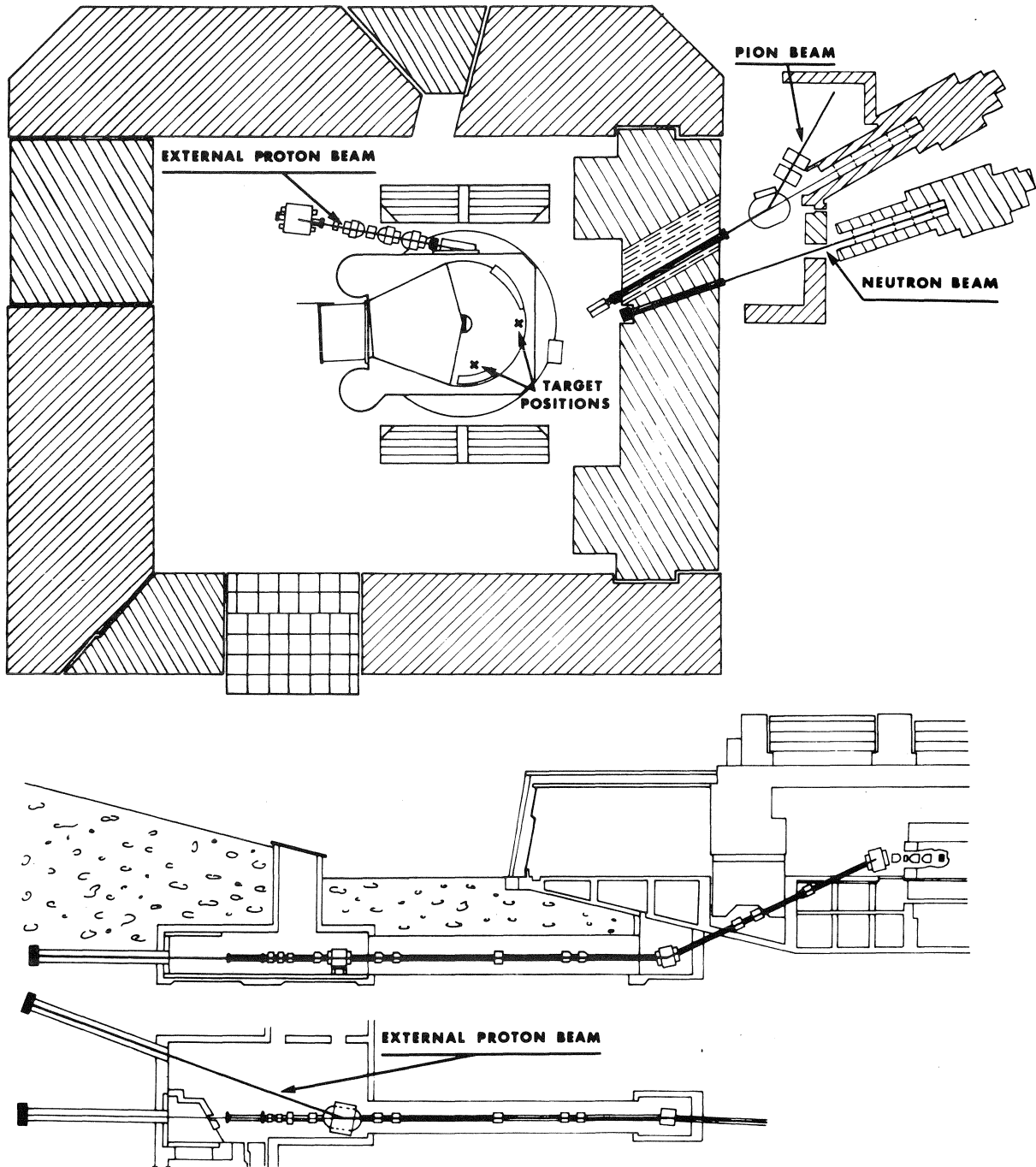


FIG. 1

# Dose variation with depth in beams

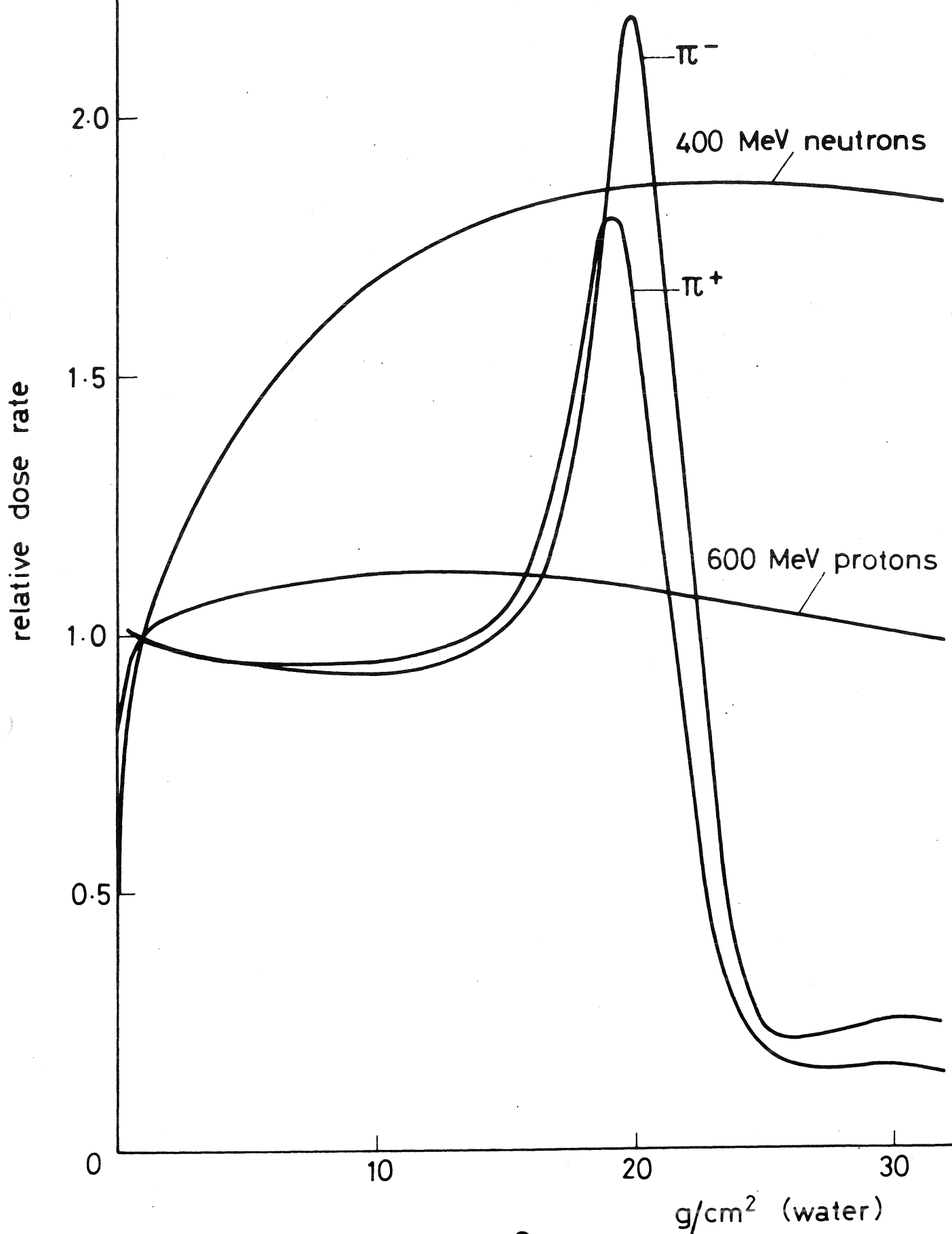
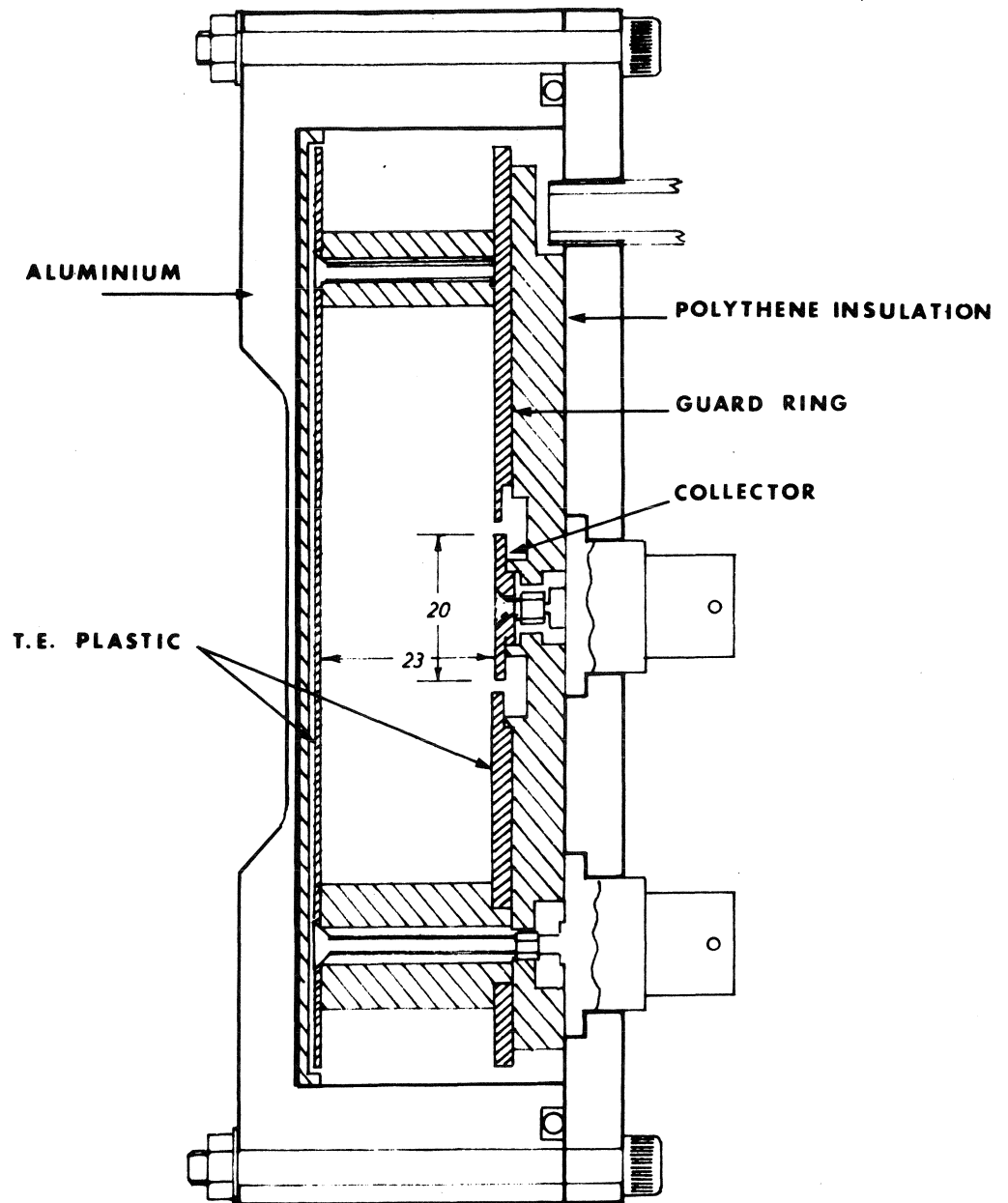


Fig. 2



**DESIGN OF A BEAM DOSEMETER**

**FIG. 3**

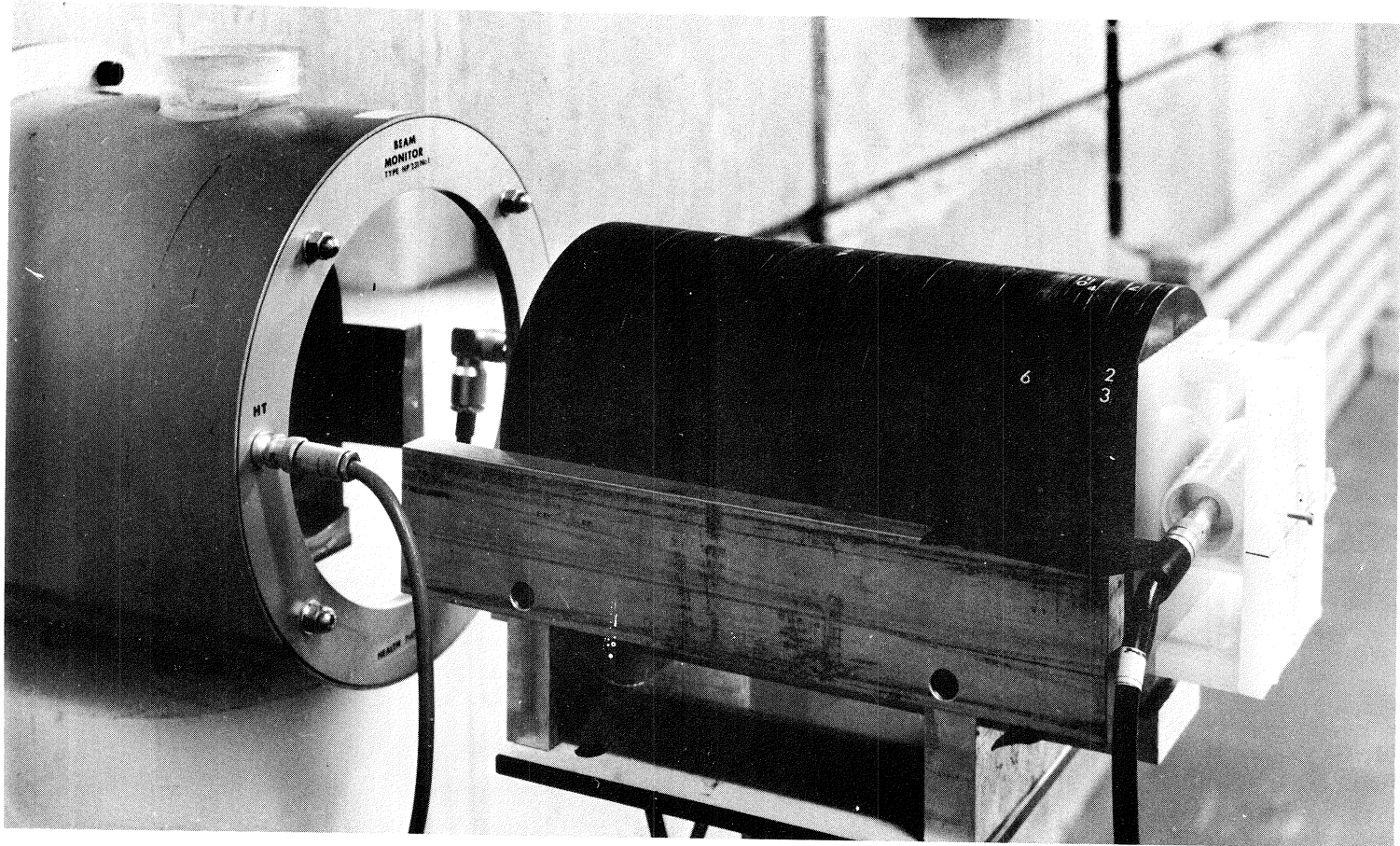


Fig. 4